

Aspergillus fumigatus SidA Is a Highly Specific Ornithine Hydroxylase with Bound Flavin Cofactor[†]

Samuel W. Chocklett and Pablo Sobrado*

Department of Biochemistry, Virginia Tech, Blacksburg, Virginia 24061

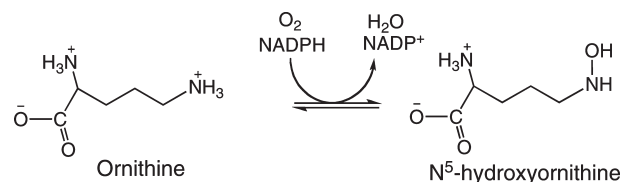
Received February 26, 2010; Revised Manuscript Received July 2, 2010

ABSTRACT: Ferrichrome is a hydroxamate-containing siderophore produced by the pathogenic fungus *Aspergillus fumigatus* under iron-limiting conditions. This siderophore contains N⁵-hydroxylated L-ornithines essential for iron binding. *A. fumigatus* siderophore A (*Af* SidA) catalyzes the flavin- and NADPH-dependent hydroxylation of L-ornithine in ferrichrome biosynthesis. *Af* SidA was recombinantly expressed and purified as a soluble tetramer and is the first member of this class of flavin monooxygenases to be isolated with a bound flavin cofactor. The enzyme showed typical saturation kinetics with respect to L-ornithine while substrate inhibition was observed at high concentrations of NADPH and NADH. Increasing amounts of hydrogen peroxide were measured as a function of reduced nicotinamide coenzyme concentration, indicating that inhibition was caused by increased uncoupling. *Af* SidA is highly specific for its amino acid substrate, only hydroxylating L-ornithine. An 8-fold preference in the catalytic efficiency was determined for NADPH compared to NADH. In the absence of substrate, *Af* SidA can be reduced by NADPH, and a C4a-(hydro)-peroxyflavin intermediate is observed. The decay of this intermediate is accelerated by L-ornithine binding. This intermediate was only stabilized by NADPH and not by NADH, suggesting a role for NADP⁺ in the stabilization of intermediates in the reaction of *Af* SidA. NADP⁺ is a competitive inhibitor with respect to NADPH, demonstrating that *Af* SidA forms a ternary complex with NADP⁺ and L-ornithine during catalysis. The data suggest that *Af* SidA likely proceeds by a sequential kinetic mechanism.

Aspergillus fumigatus is the most common opportunistic human fungal pathogen and is responsible for invasive pulmonary diseases, particularly among immunocompromised patients. *A. fumigatus* infections have become the leading cause of death in persons with leukemia and bone marrow transplants as well as patients suffering from bronchopulmonary disorders such as asthma, cystic fibrosis, and tuberculosis (1, 2). The antifungal drugs amphotericin B and itraconazole have been used to combat invasive *Aspergillus* infections; however, even with current treatment options, the mortality rate can be as high as 90% (3). Therefore, new treatments to combat pathogenic fungi are urgently needed.

Potential avenues for intervention against microbial pathogens include blocking the mechanisms of acquisition of essential nutrients during infection (4). Iron is essential for bacterial and fungal growth, but in mammals it is sequestered by iron-binding proteins such as ferritin and lactoferritin, thereby decreasing the concentration of free iron to levels unsuitable for sustaining microbial infections (5). To overcome iron deficiencies during infection, many pathogens, including *A. fumigatus*, have developed mechanisms to scavenge iron from infected hosts. Such systems include reductive iron assimilation and siderophore biosynthesis (5). For example, ferrichrome, a hydroxamate containing siderophore, is produced only under iron-limiting

Scheme 1: Reaction Catalyzed by *Af* SidA



conditions and contributes to the virulence of *A. fumigatus*. Ferrichrome biosynthesis requires the incorporation of the L-ornithine derivative N⁵-hydroxyornithine into the backbone of the siderophore where it directly coordinates the iron (6, 7). L-Ornithine hydroxylation is catalyzed by *Af* SidA,¹ a flavin-dependent monooxygenase that requires NADPH for activity (Scheme 1) (8). There is no biochemical information available for *Af* SidA; however, *in vivo* studies indicate that this enzyme is important in fungal growth and infection. *Af sidA* knockout mutants are unable to produce ferrichrome and become avirulent in murine models, suggesting that *Af* SidA is essential for pathogenesis (8, 9). Similarly, deletion of the L-ornithine hydroxylase gene in *Pseudomonas aeruginosa* and *Burkholderia cepacia* leads to attenuated virulence in these pathogens (10–12). These data indicate that the L-ornithine hydroxylase from *A. fumigatus* and other microbial pathogens represent potential drug targets.

[†]This work was supported in part by the Allan T. Gwathmey Chemistry award from the Virginia Academy of Sciences, the Ralph Powe Junior Faculty Enhancement award from the Oak Ridge Associated Universities, and the Fralin Life Science Institute.

*To whom correspondence should be addressed. Phone: (540) 231-9485. Fax: (540) 231-9070. E-mail: psobrado@vt.edu.

¹Abbreviations: *Af* SidA, N⁵-ornithine hydroxylase from *Aspergillus fumigatus*; DEAE, diethylaminoethyl; TCEP, tris(2-carboxyethyl)phosphine; IMAC, immobilized metal affinity chromatography; IPTG, isopropyl β-D-1-thiogalactopyranoside; MBP, maltose binding protein; FAD, flavin adenine dinucleotide; Tev, tobacco etch virus; SDS–PAGE, sodium dodecyl sulfate–polyacrylamide gel electrophoresis.

Here, we report the biochemical characterization of *Af*SidA, including recombinant expression and purification, oligomerization, steady-state kinetics, and inhibition studies. We use this new information to propose that *Af*SidA follows a sequential kinetic mechanism similar to other flavin monooxygenases.

MATERIALS AND METHODS

Materials. DNA encoding the *A. fumigatus* strain *Af293 sidA* gene ligated into the pUC57 plasmid was obtained from GenScript Corp. (Piscataway, NJ). Enzymes used in cloning were from Promega Corp. *Escherichia coli* TOP10 and BL21T1^R cells were from Invitrogen, and the pVP55A and pVP56K plasmids were obtained from the Center for Eukaryotic Structural Genomics at the University of Wisconsin, Madison, WI. Isopropyl β -D-1-thiogalactopyranoside (IPTG) was from Gold Biotechnology, St. Louis, MO. DNA sequencing was performed at the DNA sequencing facility of the Virginia Bioinformatics Institute. Protein purification was performed on an AKTA Prime system (GE Healthcare, Lombard, IL). L-Lysine and L-ornithine, substrates, inhibitors, buffers, and salts were purchased from Thermo-Fisher Scientific and used without further purification.

Cloning of the *Af sidA* Gene. The *Af sidA* gene cloned into pUC57 with the restriction sites *PmeI* and *SgfI* at the 5' and 3' end, respectively, was digested with Flexi enzyme blend (*PmeI* and *SgfI*). The liberated gene was ligated into similarly treated pVP55A and pVP56K expression plasmids to generate either a *His₈-sidA* or *His₈-mbp-sidA* construct, respectively (13). DNA sequencing confirmed the presence of the desired gene, and the *pVP55A:sidA* or *pVP56K:sidA* plasmids were transformed into *E. coli* BL21T1^R cells for subsequent protein expression.

Protein Expression and Purification. Due to the insolubility of the *His₈-sidA* gene product, protein expression was performed using the *pVP56K:sidA* plasmid, which expresses *Af*SidA as a fusion to maltose binding protein (MBP). An overnight culture of BL21T1^R cells containing the *pVP56K:SidA* plasmid was used to inoculate six 1.5 L flasks of Luria-Bertani (LB) broth supplemented with kanamycin (50 μ g/mL). Cultures were grown with shaking at 37 °C to an OD₆₀₀ of ~0.6. To initiate protein expression, 150 μ M IPTG was added. After 4 h of induction, cells were harvested by centrifugation and stored at -80 °C. Cells were resuspended in buffer A (25 mM HEPES, 300 mM NaCl, 25 mM imidazole, pH 7.5). The cell suspension was incubated at 4 °C in the presence of 25 μ g/mL each of DNase I, RNase, and lysozyme. All subsequent steps were performed at 4 °C. Cells were lysed by sonication, and the resultant lysate was clarified by centrifugation (34500g for 45 min). The clarified lysate was loaded onto three in-tandem 5 mL HisTrap columns (GE Healthcare) equilibrated with buffer A. The column was washed with buffer A, and *Af*SidA was eluted with a 200 mL imidazole gradient (25–300 mM) at a flow rate of 5 mL/min. Fractions containing His₈-MBP-*Af*SidA (as judged by SDS-PAGE) were pooled, diluted with buffer A, and concentrated to a 50 mL volume using an Amicon stirred cell concentrator (Billerica, MA). *Af*SidA was liberated from the His₈-MBP tag by the addition of tobacco etch virus (His₈-Tev) protease. After overnight incubation at 4 °C, the protein solution was subjected to centrifugation (34500g for 15 min) to remove traces of precipitate. The resulting sample was diluted 5-fold in buffer A and loaded onto two in-tandem 5 mL HisTrap columns equilibrated with buffer A. His₈-MBP, His₈-Tev, and His₈ peptide bind to the column, while the liberated *Af*SidA elutes in the

flow-through. The sample was pooled and concentrated to a 2 mL volume using a stirred cell concentrator. After removal of traces of precipitate by centrifugation, the sample was diluted with buffer C (25 mM HEPES, pH 7.5) and loaded onto a DEAE column equilibrated with buffer C. *Af*SidA was eluted with a 200 mL NaCl gradient (10–400 mM) at a flow rate of 5 mL/min. As the last step, fractions containing *Af*SidA were pooled and concentrated to a 1 mL volume. Approximately 50 μ L aliquots were frozen in liquid nitrogen prior to storage at -80 °C.

Determining the Extinction Coefficient of *Af*SidA. In a 1 mL cuvette, *Af*SidA was mixed with 100 mM potassium phosphate, pH 7.5. After recording the spectrum, the entire 1 mL sample was removed, and the protein was incubated at 95 °C for 1 min. The resulting solution was then centrifuged at 5000 rpm for 5 min. The supernatant was removed, and the amount of liberated FAD was determined. An extinction coefficient at 450 nm of 13700 M⁻¹ cm⁻¹ was calculated for *Af*SidA from the known extinction coefficient of free FAD (ϵ_{450} : 11.3 mM⁻¹ cm⁻¹).

Gel Filtration Chromatography. *Af*SidA (9.3 mg/mL) was loaded onto a Superdex S-75 column (GE Healthcare) equilibrated with buffer A and a final TCEP concentration of 300 μ M. Aprotinin (6500 Da), ribonuclease A (13700 Da), ovalbumin (43000 Da), conalbumin (75000 Da), aldolase (158000 Da), and ferritin (440000 Da) were used to determine the molecular mass of *Af*SidA in solution.

Product Formation Assay. The amount of hydroxylated product formed by *Af*SidA was assayed by a variation of the Csaky iodine oxidation reaction (14). The standard assay buffer contained 100 mM potassium phosphate, pH 7.5, and L-ornithine. *Af*SidA (2.0 μ M) was incubated in 92 μ L of assay buffer at 25 °C before the reaction was initiated by the addition of 1 mM NAD(P)H. The reaction proceeded for 10 min at 25 °C with shaking. The reaction was terminated by addition of 52.5 μ L of 0.2 N perchloric acid. For each L-ornithine concentration, 62.5 μ L of the terminated reaction mixture was transferred into a 0.5 mL microcentrifuge tube, and the reaction mixture was neutralized by the addition of 62.5 μ L of 5% (w/v) sodium acetate solution. To each tube, 62.5 μ L of 1% (w/v) sulfanilic acid in 25% (v/v) acetic acid and 25 μ L of 1.3% (w/v) potassium iodide in glacial acetic acid were added, and the reaction was incubated with shaking at 25 °C for 7 min. Excess iodine was removed with 25 μ L of 0.1 N sodium thiosulfate, and the color was developed by adding 25 μ L of 0.6% (w/v) α -naphthylamine in 30% (v/v) acetic acid. The absorbance at 562 nm was measured after 15 min on a SpectraMax M5e plate reader (Molecular Devices, Sunnyvale, CA). A hydroxylamine hydrochloride standard curve was used to calculate the amount of hydroxylated product produced.

Oxygen Consumption Assay. The amount of molecular oxygen consumed by *Af*SidA was monitored using a Hansatech Oxygraph (Norfolk, England). The standard assay consisted of 100 mM phosphate, pH 7.5. *Af*SidA (2.0 μ M) was incubated in 439 μ L of buffer at 25 °C before the reaction was initiated by the addition of substrates. The reaction proceeded for 1 min at 25 °C with constant stirring.

Detection of Hydrogen Peroxide. The procedure described by Hildebrandt et al. was used with minor modifications (15). The standard assay buffer was the same as described for the hydroxylation assay. The amount of hydrogen peroxide formed was determined as a function of L-ornithine (0–13 mM) and reduced nicotinamide coenzyme concentrations (0.05–6.0 mM).

The 104 μL reaction was initiated by the addition of *Af* SidA (2.0 μM). After an initial 9 min reaction, an equal volume of 3% (w/v) trichloroacetic acid was added to the sample. The terminated reaction was clarified by centrifugation (2600g for 5 min). The resulting solution was transferred to a clean 0.5 mL microcentrifuge tube and treated with 82 μL of 10 mM ferrous ammonium sulfate, followed by 26 μL of 2.5 M potassium thiocyanate. The mixture was incubated for 10 min at 25 $^{\circ}\text{C}$ with shaking, at which time the absorbance at 480 nm was recorded. A hydrogen peroxide standard curve was used to calculate the amount of hydrogen peroxide produced by *Af* SidA.

Inhibition Studies. The effects of the oxidized coenzyme NADP^+ (0–50 μM) were measured using the product formation or oxygen consumption assays. The reaction conditions were 2 μM *Af* SidA in 100 mM potassium phosphate, pH 7.5, buffer with varying NADPH concentrations and 15 mM L-ornithine.

Mass Spectrometry. For mass spectral analysis of *Af* SidA, a portion of the protein was desalted using an OMIX C18 tip (Varian, Inc., Lake Forest, CA) following the manufacturer's directions. Then, *Af* SidA (approximately 125 μM) was mixed with 10 mg/mL sinapinic acid (Aldrich) in acetonitrile/water (30:70) supplemented with 0.1% trifluoroacetic acid. A 1 μL aliquot was spotted onto a MALDI target plate and allowed to air-dry. The sample was analyzed in the linear positive ion-operating mode using an ABI 4800 MALDI TOF/TOF.

Data Analysis. Kinetic data were analyzed using the programs KaleidaGraph (Synergy, Reading, PA) and EnzFitter (BioSoft, Cambridge, U.K.). Initial rate data were fit to the Michaelis–Menten equation to obtain k_{cat} and K_{m} values. The substrate inhibition constant for reduced nicotinamide coenzyme (K_{is}) was determined by fitting the data to eq 1. Inhibition data with NADP^+ were fit to eq 2, which describes competitive inhibition where K_{is} is the inhibition constant.

$$v = \frac{k_{\text{cat}}S}{K_{\text{m}} + S + S^2/K_{\text{is}}} \quad (1)$$

$$v = \frac{k_{\text{cat}}S}{K_{\text{m}} \left(1 + \frac{1}{[K_{\text{is}}]} \right) + S} \quad (2)$$

RESULTS

Protein Expression and Purification. Recombinant *Af* SidA was expressed as a fusion to MBP containing an 8 \times His tag at the N-terminus (8 \times His-MBP) in *E. coli* BL21T1^R cells. Expression trials with the N-terminal 8 \times His tag produced recombinant protein that was present in the insoluble fraction (data not shown). Recombinant 8 \times His-MBP-*Af* SidA was purified from cells induced for 4 h by three chromatographic steps with a yield of 15 mg of highly active enzyme/L of culture (Figure 1). The UV–visible absorbance spectrum indicates the presence of flavin cofactor bound to the purified enzyme with peaks at 380 and 450 nm. This is the first report of the isolation of a member of the microbial N-hydroxylating monooxygenases containing bound flavin cofactor. The stoichiometry of flavin incorporation was determined to be 50–65%. This was determined by dividing the protein concentration calculated using the flavin extinction coefficient by the protein concentration using the Bradford assay.

Gel Filtration Chromatographic and Mass Spectrometric Analyses. From the SDS–PAGE analysis of purified recombinant *Af* SidA, the molecular mass of this protein was estimated to

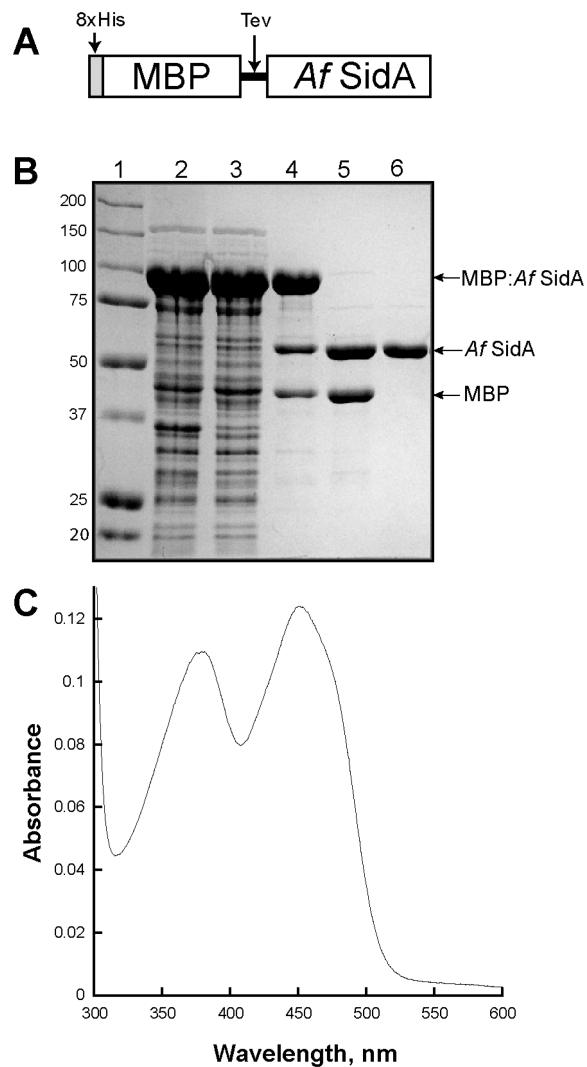


FIGURE 1: Summary of *Af* SidA purification. (A) Schematic of the pVP56K vector. (B) SDS–PAGE gel summarizing the purification of *Af* SidA: lane 1, molecular mass markers; lane 2, crude lysate; lane 3, lysate supernatant; lane 4, sample after IMAC step; lane 5, sample after treatment with Tev protease to remove *Af* SidA from MBP; lane 6, final sample after DEAE chromatography. (C) UV–visible spectrum of bound FAD in purified *Af* SidA.

Table 1: Solution Molecular Weight and Mass Spectrometry Studies of *Af* SidA

| sample | technique | calcd MW (Da) | obsd MW (Da) |
|-----------------------|----------------|---------------|--------------|
| <i>Af</i> SidA | MALDI-TOF MS | 57231 | 57210 |
| <i>Af</i> SidA | SDS–PAGE | 57231 | 55000 |
| <i>Af</i> SidA (soln) | gel filtration | 232064 | 228000 |
| FAD | MALDI-TOF MS | 785.55 | 786 |

be ~ 55 kDa. A more precise molecular mass of 57210 Da was determined by mass spectrometry analysis. This is in agreement with the predicted molecular mass of 57231 Da based on the amino acid sequence. The estimated solution molecular mass of *Af* SidA was 228 kDa, as determined by gel filtration, suggesting that the enzyme adopts a tetrameric quaternary structure. Mass spectral analysis identified the cofactor as FAD (Table 1).

Enzyme Activity Varying L-Ornithine. At a constant concentration (1 mM) of NADPH, *Af* SidA hydroxylated L-ornithine with an apparent k_{cat} of $29 \pm 0.3 \text{ min}^{-1}$, which is consistent

Table 2: Steady-State Kinetic Parameters Determined by Following the Formation of Hydroxylated Ornithine^a

| substrate | $k_{\text{cat}}, \text{min}^{-1}$ | K_{m}, mM | $k_{\text{cat}}/K_{\text{m}}, \text{min}^{-1} \text{mM}^{-1}$ | K_{I}, mM |
|------------------------|-----------------------------------|---------------------------|---|---------------------------|
| ornithine ^b | 30 ± 1 | 1.7 ± 0.14 | 18 ± 0.1 | |
| ornithine ^c | 29 ± 0.3 | 1.70 ± 0.06 | 17 ± 0.4 | |
| NADPH ^d | 75 ± 9 | 0.94 ± 0.17 | 79 ± 17 | 2.8 ± 0.6 |
| NADH ^d | 71 ± 16 | 0.90 ± 0.30 | 79 ± 31 | 1.9 ± 0.7 |

^aConditions: 100 mM potassium phosphate at pH 7.5 and 25 °C. ^bNADH was kept constant at 1 mM. ^cNADPH was kept constant at 1 mM. ^dL-Ornithine concentration was saturating at 15 mM.

with published values of other ornithine hydroxylases (10, 16). In contrast, the k_{cat} value determined using the oxygen consumption assay was 79% higher than the k_{cat} value determined using the product formation assay. Similarly, at a constant concentration of NADH (1 mM), *Af*SidA displayed the same k_{cat} value as with NADPH using the product formation assay. However, using the oxygen consumption assay with NADH, the k_{cat} value was 36% higher than the value calculated following the product formation assay (Table 3). The K_{m} value for L-ornithine had the same value irrespective of whether saturated concentrations of NADPH or NADH were used. With NADPH, the K_{m} value calculated using the oxygen consumption assay was ~3.4-fold lower than the K_{m} value calculated with the product formation assay, while the K_{m} value was almost the same in either assay using NADH.

Enzyme Activity Varying Reduced Nicotinamide Coenzyme Concentrations. By measuring the rate of product formation when varying NADPH or NADH, it was observed that as the concentration was increased above ~1 mM, the rate decreased, indicative of substrate inhibition. The calculated kinetic parameters with both nicotinamide coenzymes are almost identical (Table 2). In contrast, different results were observed when the activity of *Af*SidA was determined by measuring the rate of oxygen consumption at various reduced nicotinamide coenzyme concentrations. As shown in Figure 2, no apparent substrate inhibition was observed with either NADPH or NADH. Furthermore, the $k_{\text{cat}}/K_{\text{m}}$ value for NADPH was 8-fold higher than for NADH. This higher catalytic efficiency for NADPH originated from a lower K_{m} value for this substrate (Table 3).

Hydrogen Peroxide Formation. The possibility that not every molecule of oxygen consumed by *Af*SidA was channeled toward product formation was tested by determining if hydrogen peroxide was produced during turnover. Figure 3 illustrates the production of hydrogen peroxide, as a function of both L-ornithine and reduced nicotinamide coenzyme concentration. Here, it was seen that hydrogen peroxide formation decreased as a function of L-ornithine concentration in the presence of either NADH or NADPH, ranging from 50 to 25 μmol produced with NADPH and from 195 to 45 μmol produced with NADH. Conversely, the amount of hydrogen peroxide increased as a function of reduced nicotinamide coenzyme, ranging from 5 to 60 μmol produced with NADPH and from 12 to 135 μmol produced with NADH. These results suggest that NADPH is the preferred substrate for this reaction, since a higher degree of coupling is observed.

Oxygen Activation by Substrate and Analogues. To further explore the reactivity of *Af*SidA, the rates of product formation and oxygen consumption of *Af*SidA were measured after the addition of L-ornithine, as well as a series of structurally

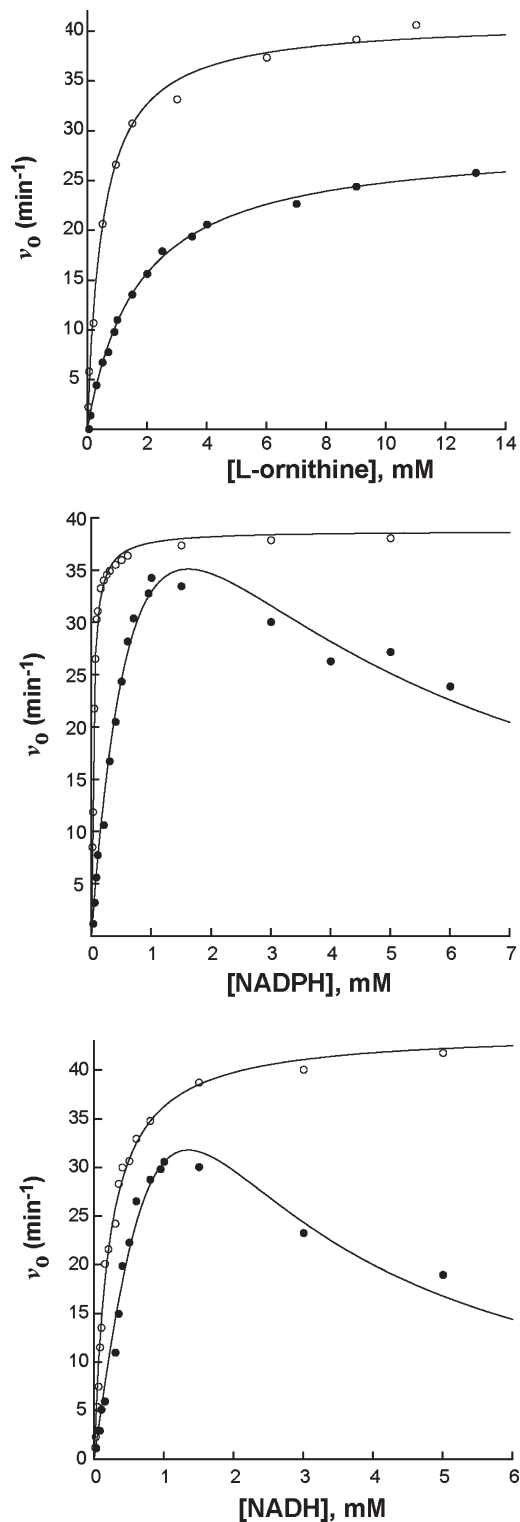


FIGURE 2: Substrate and reduced nicotinamide coenzyme saturation curves as determined by the product formation and oxygen consumption assays. (A) Substrate saturation curves using the product formation (●) and oxygen consumption (○) assays. (B) Reduced nicotinamide coenzyme saturation curves using NADPH using the product formation (●) and oxygen consumption (○) assays. (C) The same as (B) but with NADH instead of NADPH.

related compounds. These results are presented in Table 4. *Af*SidA reacts only very slowly with molecular oxygen in the presence of NADPH and the absence of L-ornithine. However, upon the addition of L-ornithine, the rate of oxygen consumption increased 27-fold over the rate in the absence of L-ornithine

Table 3: Steady-State Kinetic Parameters Determined by Following the Rate of Oxygen Consumption^a

| substrate | k_{cat} , min^{-1} | K_m , mM | k_{cat}/K_m , $\text{min}^{-1} \text{mM}^{-1}$ |
|------------------------|--------------------------------------|------------------|---|
| ornithine ^b | 41 ± 0.8 | 0.5 ± 0.05 | 80 ± 6 |
| ornithine ^c | 52 ± 2 | 2.0 ± 0.1 | 26 ± 1 |
| NADPH ^d | 38 ± 0.5 | 0.03 ± 0.002 | 1263 ± 88 |
| NADH ^d | 44 ± 0.8 | 0.21 ± 0.01 | 205 ± 9 |

^aConditions: 100 mM potassium phosphate at pH 7.5 and 25 °C. ^bAssay was done using 1 mM NADH. ^cNADPH was kept constant at 1 mM. ^dOrnithine was kept constant at 15 mM.

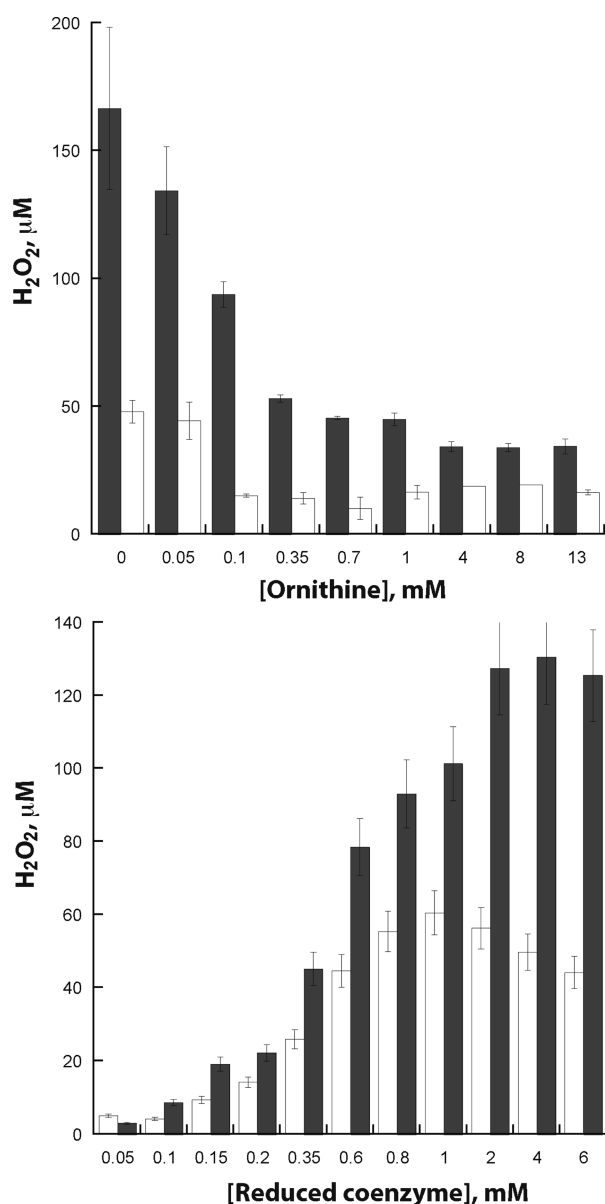


FIGURE 3: H₂O₂ production by *AfSidA* as a function of ornithine and reduced nicotinamide coenzyme. The amounts of H₂O₂ produced were measured for NADPH (solid bars) and NADH (open bars).

(Figure 4). Conversely, L-arginine, L-cysteine, histamine, L-norvaline, L-serine, and tryptamine did not stimulate the rate of oxygen consumption, and no hydroxylated product was formed. Interestingly, oxygen consumption was increased 17-fold upon the addition of L-lysine, although no hydroxylated product was formed. Thus, L-lysine enhances the oxidase activity of *AfSidA* but does not serve as an appropriate substrate.

Table 4: *AfSidA* Substrate Specificity^a

| substrate | rate, min^{-1} | |
|--------------|-------------------------|--------------------------|
| | product formation assay | oxygen consumption assay |
| +L-ornithine | 29 ± 0.3 | 41 ± 0.8 |
| -L-ornithine | | 1.5 ± 0.1 |
| +L-lysine | | 26 ± 3.5 |

^aStandard conditions were the same as indicated in Tables 2 and 3. The assays were done in the presence of 0.5 mM NADPH. L-Lysine and L-ornithine were tested at 15 mM. Similarly, 15 mM of L-arginine, L-cysteine, L-histamine, L-norvaline, L-serine, and L-tryptamine were also tested as possible substrates and neither hydroxylated product nor an increase in the rate of oxygen consumption were detected.

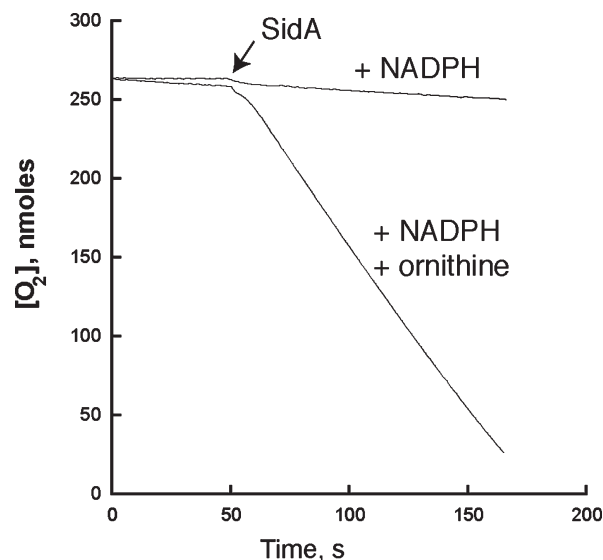


FIGURE 4: Traces from the oxygen consumption assay demonstrating the low oxidase activity in the absence of substrate and the activation by L-ornithine binding. The reaction was performed in potassium phosphate buffer, pH 7.5, and 1 mM NADPH, in the absence or presence of 15 mM L-ornithine.

Oxygenated Flavin Intermediates. Changes in the flavin spectrum of *AfSidA* were monitored using an Agilent 8453 photodiode array spectrophotometer. In a 1 mL cuvette, excess amounts of NADPH (2-fold) and NADP⁺ (3-fold) were mixed with *AfSidA* in aerobic 100 mM potassium phosphate, pH 7.5. A spectrum with a peak at 366 nm was detected (Figure 5). This spectrum decayed to the oxidized flavin within 3 min. In separate experiments, NADPH was substituted with NADH, and no transient intermediates were seen.

Inhibition Studies. Using the oxygen consumption assay, the effect of different concentrations of NADP⁺ against NADPH was determined. The resulting rates, plotted as double reciprocal plots, clearly show that NADP⁺ is a competitive inhibitor against NADPH, since the lines were not parallel but intersected at the y-axis (Figure 6). The calculated inhibition constant was $590 \pm 18 \mu\text{M}$.

DISCUSSION

Flavin-dependent monooxygenases are a group of enzymes capable of catalyzing epoxidations, Baeyer–Villiger oxidations, and hydroxylations on hydrocarbons and sulfur- and nitrogen-containing molecules (17, 18). Among the members of this family, the least studied are the N-hydroxylating monooxygenases

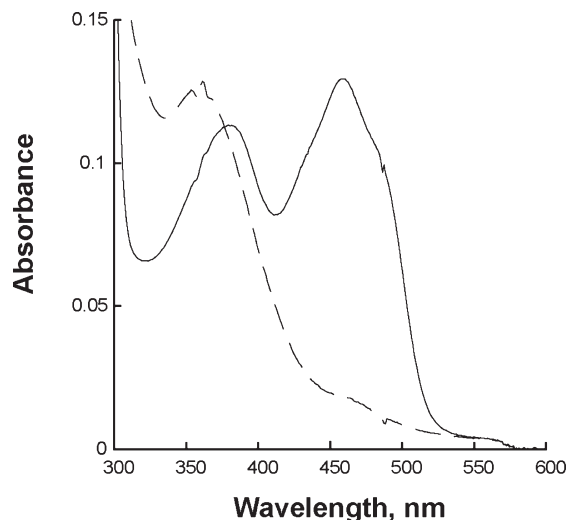


FIGURE 5: Detection of a stable C4a-flavin peroxide by *Af SidA*. Upon addition of a 2-fold excess of NADPH to oxidized *Af SidA*, UV-visible traces indicate the rapid formation of a stable (hydro)-peroxyflavin intermediate necessary for catalysis.

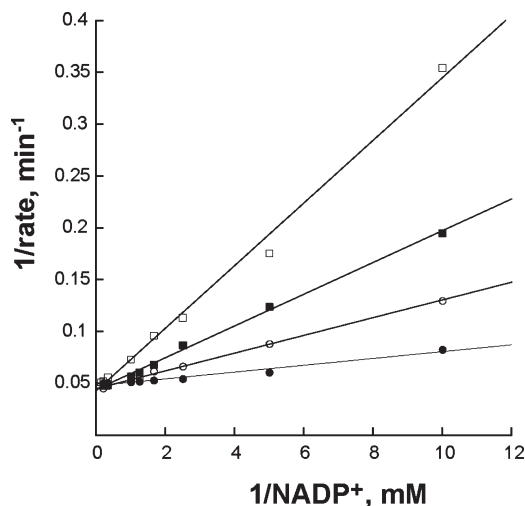
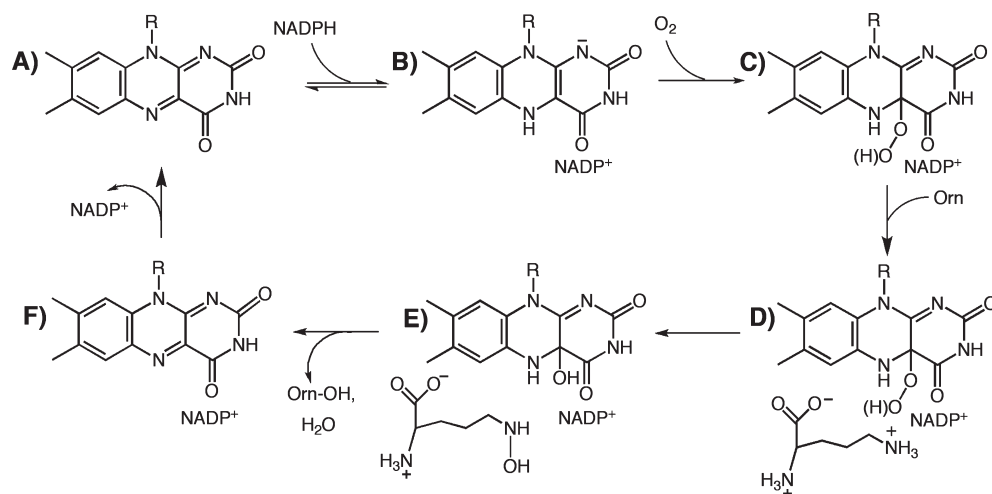


FIGURE 6: Inhibition of *Af SidA* by NADP^+ as determined by the oxygen consumption assay. Double reciprocal plots of rates as a function of NADPH concentration. NADP^+ concentrations used were (●) 0 mM, (○) 500 μM , (■) 1 mM, and (□) 2 mM.

Scheme 2: Proposed Kinetic Mechanism for *Af SidA*



(NMOs) (18). NMOs play an essential role in siderophore-mediated iron trafficking in many microbes, including several human pathogens. Specifically, NMOs hydroxylate the amino group on the side chains of L-lysine and L-ornithine, leading to the formation of a hydroxamate that comprises the iron-binding site in siderophores such as mycobactin in *M. tuberculosis* and ferrichrome in *A. fumigatus* (5, 8, 19). Previous mechanistic studies of NMOs were hindered by protein instability and weak binding of the flavin cofactor in the recombinantly produced enzymes (20–22). Here, we report the characterization of *Af SidA*, an N^5 -ornithine hydroxylase from *A. fumigatus*. The recombinant protein was isolated for the first time in a stable form and, more importantly, with a bound flavin cofactor. It was required that the protein be expressed as a fusion to MBP, and after separation from MBP, the protein remained soluble and could be purified to homogeneity (Figure 1).

Af SidA reacts with NADPH in the absence of L-ornithine, indicating that this substrate is not required to be bound to the oxidized enzyme before NADPH binding and hydride transfer (Figure 4). Furthermore, in the absence of L-ornithine, NADPH-reduced *Af SidA* reacts with molecular oxygen forming a C4a-(hydro)peroxyflavin intermediate (Figure 5). In the presence of L-ornithine, the rate of flavin reoxidation was significantly accelerated, indicating that the C4a-(hydro)peroxyflavin awaits amino acid substrate binding to complete turnover (Figures 4 and 5). These results provide insight about the kinetic mechanism of *Af SidA* (Scheme 2). The first step is reduction of the flavin by NAD(P)H followed by reaction with molecular oxygen to form the C4a-oxygenated species, in the absence of L-ornithine (Scheme 2A–C). The C4a-hydroperoxyflavin is expected to be the intermediate involved in substrate hydroxylation; further experiments need to be performed to determine the exact nature of the oxygenated species observed in *Af SidA*. However, it is clear that upon L-ornithine binding (Scheme 2D) the enzyme rapidly turns over forming N^5 -hydroxyornithine and the predicted C4a-hydroxyflavin (Scheme 2E). NADP^+ was shown to be a competitive inhibitor versus NADPH, indicating that this product remains bound during catalysis and is the last product to be released (Scheme 2F). These results are consistent with a sequential kinetic mechanism for the catalytic cycle of *Af SidA*. This is consistent with the kinetic mechanisms determined for related flavoenzymes such as hog liver flavin monooxygenase,

phenyl-acetone monooxygenase (PAMO), and N^5 -ornithine hydroxylase from *P. aeruginosa* (PvdA) (16, 23, 24).

The well-known role of NADPH during catalysis of flavin-dependent monooxygenases is to provide reducing equivalents to FAD (18). Bound $NADP^+$ has been shown to play other roles during catalysis. For example, in the structure of flavin monooxygenase from *Methylophaga* sp. strain SK1, $NADP^+$ is found in a nonoptimal position for hydride transfer. The binding mode suggests that $NADP^+$ might directly interact with the C4a-hydroxyflavin intermediate (25). Similarly, dual roles for $NADP^+$ have been proposed in PAMO, where $NADP^+$ stabilizes the C4a-peroxyflavin intermediate and is the last substrate to exit the active site. As described above, *Af* SidA readily utilizes NADPH for reducing equivalents, and $NADP^+$ stabilizes the C4a-(hydro)peroxyflavin intermediate. These findings suggest that in *Af* SidA $NADP^+$ might also play a role in the stabilization of flavin intermediates (Scheme 2). The mechanism of hydroxylation in PvdA was recently proposed to include protonation of the C4a-peroxyflavin by the amino group being hydroxylated in L-ornithine (26). Although this is an attractive proposal, the fact that L-lysine can stimulate the oxidase activity of *Af* SidA, but is not hydroxylated, indicates that this is not the mechanism followed by *Af* SidA. If L-lysine is in close enough proximity to protonate the C4a-peroxyflavin, there should be some level of hydroxylation. *Af* SidA was shown to be highly specific for the hydroxylation of ornithine. However, the binding of lysine and excess NADH or NADPH modulated the activity of the enzyme (Figure 3 and Table 4). Concentrations of reduced coenzyme higher than 1 mM induced uncoupling in the reaction. Lysine binding enhanced the oxidase activity, effectively consuming NAD(P)H and producing hydrogen peroxide. Identification of compounds that mimic the action of lysine and excess NAD(P)H binding (e.g., inhibit ornithine hydroxylation and enhance hydrogen peroxide production) might serve as effective drugs for the treatment of *A. fumigatus* infections.

ACKNOWLEDGMENT

We thank Drs. Rich Helm and Keith Ray for the MS analysis and Jenna Hess for help in the purification of *Af* SidA. We also thank Drs. Janet Webster and Michael Klemba for critical reading of the manuscript.

REFERENCES

- Marr, K. A., Patterson, T., and Denning, D. (2002) Aspergillosis. Pathogenesis, clinical manifestations, and therapy. *Infect. Dis. Clin. North. Am.* 16, 875–894, vi.
- Denning, D. W. (2002) Echinocandins: a new class of antifungal. *J. Antimicrob. Chemother.* 49, 889–891.
- Tekaia, F., and Latge, J. P. (2005) *Aspergillus fumigatus*: saprophyte or pathogen? *Curr. Opin. Microbiol.* 8, 385–392.
- Frederick, R. E., Mayfield, J. A., and DuBois, J. L. (2009) Iron trafficking as an antimicrobial target. *Biometals* 22, 583–593.
- Fischbach, M. A., Lin, H., Liu, D. R., and Walsh, C. T. (2006) How pathogenic bacteria evade mammalian sabotage in the battle for iron. *Nat. Chem. Biol.* 2, 132–138.
- Rementeria, A., Lopez-Molina, N., Ludwig, A., Vivanco, A. B., Bikandi, J., Ponton, J., and Garaizar, J. (2005) Genes and molecules involved in *Aspergillus fumigatus* virulence. *Rev. Iberoam. Micol.* 22, 1–23.
- Haas, H. (2006) Fungal siderophores: their role in disease. *Annu. Rev. Phytopathol.* 46, 149–187.
- Hissen, A. H., Wan, A. N., Warwas, M. L., Pinto, L. J., and Moore, M. M. (2005) The *Aspergillus fumigatus* siderophore biosynthetic gene *sidA*, encoding L-ornithine N^5 -oxygenase, is required for virulence. *Infect. Immun.* 73, 5493–5503.
- Schrettl, M., Bignell, E., Kragl, C., Sabiha, Y., Loss, O., Eisendle, M., Wallner, A., Arst, H. N., Jr., Haynes, K., and Haas, H. (2007) Distinct roles for intra- and extracellular siderophores during *Aspergillus fumigatus* infection. *PLoS Pathog.* 3, 1195–1207.
- Visca, P., Serino, L., and Orsi, N. (1992) Isolation and characterization of *Pseudomonas aeruginosa* mutants blocked in the synthesis of pyoverdine. *J. Bacteriol.* 174, 5727–5731.
- Sokol, P. A., Darling, P., Woods, D. E., Mahenthalingam, E., and Kooi, C. (1999) Role of ornibactin biosynthesis in the virulence of *Burkholderia cepacia*: characterization of *pvdA*, the gene encoding L-ornithine $N(5)$ -oxygenase. *Infect. Immun.* 67, 4443–4455.
- Takase, H., Nitanai, H., Hoshino, K., and Otani, T. (2000) Impact of siderophore production on *Pseudomonas aeruginosa* infections in immunosuppressed mice. *Infect. Immun.* 68, 1834–1839.
- Blommel, P. G., Martin, P. A., Seder, K. D., Wrobel, R. L., and Fox, B. G. (2009) Flexi vector cloning. *Methods Mol. Biol.* 498, 55–73.
- Csaky, T. (1948) On the estimation of bound hydroxylamine in biological materials. *Acta Chem. Scand.* 450–454.
- Hildebrandt, A. G., Roots, I., Tjoe, M., and Heinemeyer, G. (1978) Hydrogen peroxide in hepatic microsomes. *Methods Enzymol.* 52, 342–350.
- Meneely, K. M., and Lamb, A. L. (2007) Biochemical characterization of a flavin adenine dinucleotide-dependent monooxygenase, ornithine hydroxylase from *Pseudomonas aeruginosa*, suggests a novel reaction mechanism. *Biochemistry* 46, 11930–11937.
- Massey, V. (2000) The chemical and biological versatility of riboflavin. *Biochem. Soc. Trans.* 28, 283–296.
- van Berkel, W. J., Kamerbeek, N. M., and Fraaije, M. W. (2006) Flavoprotein monooxygenases, a diverse class of oxidative biocatalysts. *J. Biotechnol.* 124, 670–689.
- Quadri, L. E., Sello, J., Keating, T. A., Weinreb, P. H., and Walsh, C. T. (1998) Identification of a *Mycobacterium tuberculosis* gene cluster encoding the biosynthetic enzymes for assembly of the virulence-conferring siderophore mycobactin. *Chem. Biol.* 5, 631–645.
- Stehr, M., Smau, L., Singh, M., Seth, O., Macheroux, P., Ghisla, S., and Diekmann, H. (1999) Studies with lysine N^6 -hydroxylase. Effect of a mutation in the assumed FAD binding site on coenzyme affinities and on lysine hydroxylating activity. *Biol. Chem.* 380, 47–54.
- Marrone, L., and Viswanatha, T. (1997) Effect of selective cysteine → alanine replacements on the catalytic functions of lysine: N^6 -hydroxylase. *Biochim. Biophys. Acta* 1343, 263–277.
- Dick, S., Marrone, L., Duetzel, H., Beecroft, M., McCourt, J., and Viswanatha, T. (1999) Lysine: N^6 -hydroxylase: stability and interaction with ligands. *J. Protein Chem.* 18, 893–903.
- Ziegler, D. M. (2002) An overview of the mechanism, substrate specificities, and structure of FMOs. *Drug Metab. Rev.* 34, 503–511.
- Torres Pazmino, D. E., Baas, B. J., Janssen, D. B., and Fraaije, M. W. (2008) Kinetic mechanism of phenylacetone monooxygenase from *Thermobifida fusca*. *Biochemistry* 47, 4082–4093.
- Alfieri, A., Malito, E., Orru, R., Fraaije, M. W., and Mattevi, A. (2008) Revealing the moonlighting role of NADP in the structure of a flavin-containing monooxygenase. *Proc. Natl. Acad. Sci. U.S.A.* 105, 6572–6577.
- Meneely, K. M., Barr, E. W., Bollinger, J. M., Jr., and Lamb, A. L. (2009) Kinetic mechanism of ornithine hydroxylase (PvdA) from *Pseudomonas aeruginosa*: substrate triggering of O_2 addition but not flavin reduction. *Biochemistry* 48, 4371–4376.